Los Alamos
NATIONAL LABORATORY
EST. 1943

LA-UR-16-20591
Approved for public release; distribution is unlimited.

Title: PAGOSA Sample Problem: Elastic Precursor

Author(s): Weseloh, Wayne N.
Clancy, Sean Patrick

Intended for: Report

Issued: 2016-02-03

Disclaimer:
Los Alamos National Laboratory, an affirmative action/equal opportunity employer,is operated by the Los Alamos National Security, LLC for the National NuclearSecurity Administration of the U.S. Department of Energy under contract DE-AC52-06NA25396. By approving this article, the publisher recognizes that the U.S. Government retains nonexclusive, royalty-free license to publish or reproduce the published form of this contribution, or to allow others to do so, for U.S. Government purposes. Los Alamos National Laboratory requests that the publisher identify this article as work performed under the auspices of the U.S. Departmentof Energy. Los Alamos National Laboratory strongly supports academic freedom and a researcher's right to publish; as an institution, however, the Laboratory does not endorse the viewpoint of a publication or guarantee its technical correctness.

PAGOSA

Sample Problem:

Elastic Precursor

by

Wayne N. Weseloh
Sean P. Clancy

Los Alamos National Laboratory

January 2016

This page intentionally left blank.

ELASTIC PRECURSOR

A PAGOSA simulation of a flyer plate impact which produces an elastic precursor wave is examined. The simulation is compared to an analytic theory for the Mie-Grüneisen equation of state and an elastic-perfectly-plastic strength model.

This page intentionally left blank.

ELASTIC PRECURSOR

For a material described by the Mie-Grüneisen equation of state and a perfectly-elastic-plastic strength model, it is possible to derive an exact solution to the uniaxial strain equations under a step function velocity boundary condition. An exact solution was developed in a journal article by Udaykumar *et. al.*[1] in 2003. The exact solution exhibits a two wave structure; a fast wave called the elastic precursor followed by a stronger and slower plastic shock wave. The solution predicts sharp discontinuities for the material models used.

A copper flyer plate impacts a copper target at 40 m/s. The initial setup geometry is shown in Figure P1.

Run the simulation to exactly 170 μs (about 240 cycles). Compare the analytic results with the PAGOSA simulation.

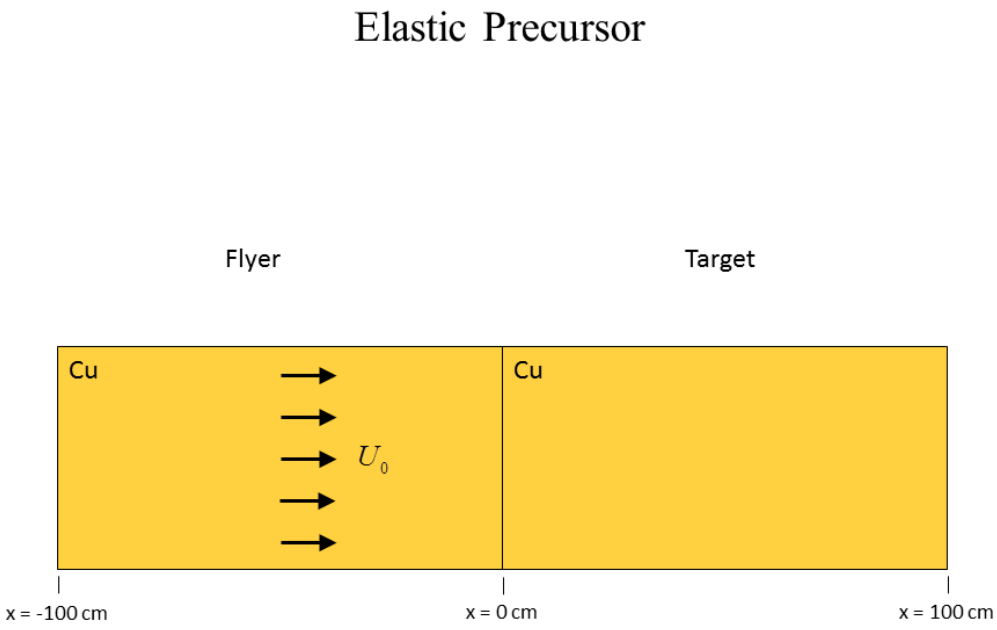

Figure P1. The geometry of the PAGOSA Elastic Precursor simulation.

[1] H.S. Udaykumar, L.Tran, D.M. Belk, and K.J. Vanden, *An Eulerian Method for Computation of Multimaterial Impact with ENO Shock-Capturing and Sharp Interfaces*, **Journal of Computational Physics**, Volume 186 (2003), pages 136-177. See section 7.2: *Impact on elasto-plastic material*, pages 155-163.

Theory

Consider a half-space of an elastic-plastic material initially at rest. At $t = 0$, the boundary of the half-space is subjected to a sudden velocity. The response of an elastic-plastic material can produce one or two shock waves, depending on the impulse velocity and the material properties.

The response of the elastic-plastic material is illustrated by a *P*-*V* diagram in Figure P2(a). The Hugoniot curve is represented by a green line. Notice the change in slope of this curve at the yield point (the Hugoniot Elastic Limit represented by the black open circle).

If the impact stress is below the Hugoniot Elastic Limit (HEL), then a single elastic wave is generated, as shown in Figure P2(b).

Now when the impact stress exceeds the HEL, then two shock waves are produced, as shown in Figure P2(c). The Rayleigh line is composed of two straight line segments with each segment having a unique slope. The elastic slope is greater than the plastic slope – the elastic wave velocity is greater than the plastic wave velocity. This is called a *splitting shock wave* because the jump in stress produced by the boundary condition produces two waves. The leading shock wave is called the *elastic precursor*. The trailing shock wave is called the *plastic shock wave*.

In Figure P2(d), the third case is illustrated. The initial state can be connected to the Hugoniot state with a single straight line. The slope of this Rayleigh line is exactly the slope of the Rayleigh line for the elastic precursor. It is often said, for this case, that the elastic precursor is overdriven by the plastic shock wave. Figure P2(d) shows the case of the transition between the two wave case and the (high stress) single wave case.

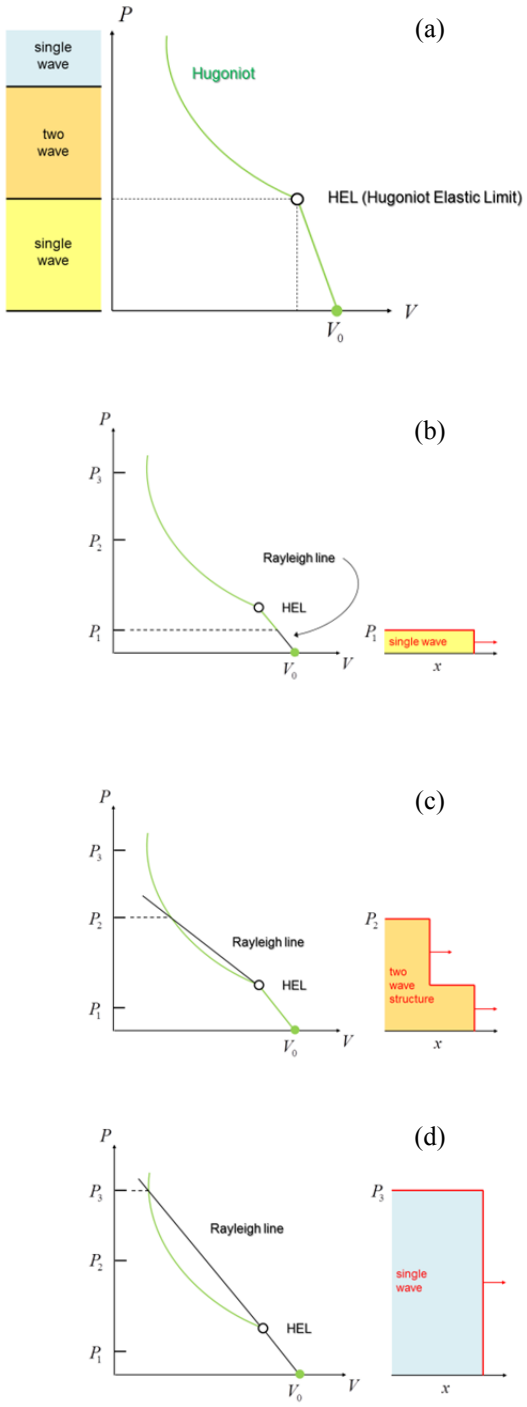

Figure P2. **(a)** Pressure versus specific volume Hugoniot curve for elastic-plastic materials. **(b)** Represents a single shock wave. **(c)** The two wave structure of interest in this sample. **(d)** The overdriven case resulting in a single shock wave.

The following derivation follows the development in Udaykumar's article[2]. The nomenclature is slightly altered to be more consistent with PAGOSA's standard style and practices. Also, several points of the derivation are expanded.

The material in this simulation is copper. The material properties are given in Table 1 below.

Table 1. Material properties of copper[3]

name	*symbol*	*value*	*units*
Mass density	ρ_0	8.93	g/cm^3
U_s / U_p intercept	c_0	0.394	cm/μs
U_s/ U_p slope	s	1.49	-
Grüneisen gamma	Γ_0	2.0	-
Shear modulus	G	0.450	Mbar
Yield stress	Y	0.90	kbar

The derivation of an exact solution to the elastic precursor begins by considering the stress state at the Hugoniot Elastic Limit. The Hugoniot Elastic Limit (HEL) is defined as the critical shock pressure at which a solid yields under uniaxial strain of a plane shock wave. The history of the term is given in Graham[4].

Below the yield stress, the deviatoric stress rate[5] is

$$\dot{S}_{xx} = 2G(\dot{e}_{xx} - \tfrac{1}{3}\nabla\cdot\mathbf{u}) = \tfrac{4}{3}G\,\nabla\cdot\mathbf{u}\,, \tag{1}$$

where the divergence, in its Lagrangian form[6], is

$$\nabla\cdot\mathbf{u} = \lim_{Vol\to 0}\frac{1}{Vol}\frac{dVol}{dt} = \frac{d}{dt}\log_e(Vol) = -\frac{d}{dt}\log_e(\rho)\,. \tag{2}$$

Integrating[7] we find that

$$S_{xx} = \tfrac{4}{3}G\log_e(\rho_0/\rho)\ . \tag{3}$$

At the yield point, designated with a superscript Y, the deviatoric stress[8] is

$$S_Y = -\tfrac{2}{3}Y = -0.6\ \text{kbar}\,, \tag{4}$$

[2] Udaykumar, *et. al.*, pages 155-157.
[3] Udaykumar, *et. al.*, page 158.
[4] R.A. Graham, **Solids under High-Pressure Shock Compression: Mechanics, Physics, and Chemistry**, Springer-Verlag Inc., New York (1993). Section 2.4 The Hugoniot Elastic Limit, pages 27-36.
[5] W.N. Weseloh, S.P. Clancy, and J.W. Painter, **PAGOSA Physics Manual**, Los Alamos National Laboratory, LA-14425-M (August 2010), Appendix A, page 167.
[6] *Ibid.*, Equation (D.6), page 182.
[7] The constant of integration is chosen such that $S_{xx}(\rho{=}\rho_0) = 0$.
[8] *Ibid.*, Section 14.3, page 134.

where the negative sign indicates compression. The density at the yield point, ρ_Y, is

$$\rho_Y = \rho_0 \exp(Y / 2G) \ . \tag{5}$$

The governing equations (Rankine-Hugoniot jump[9,10] conditions) for plane shock waves in an elastic-plastic media are

$$[\![u]\!] = \rho_0 U_{se} [\![V]\!] \ , \tag{6a}$$

$$[\![\sigma_{xx}]\!] = -\rho_0 U_{se} [\![u]\!], \text{ and} \tag{6b}$$

$$[\![E]\!] = \tfrac{1}{2} \sigma_{xx} [\![V]\!]. \tag{6c}$$

where, for example, the quantity $[\![V]\!]$ is the jump in specific volume, V. These jump conditions are the general relations for a solid. Usually these relations are shown in the simpler form without the Cauchy stress σ_{xx} .

These relations will be used to determine the elastic shock and, in turn, the plastic shock.

The thermodynamic state of the elastic precursor wave is found by solving the Mie-Grüneisen equation of state[11] for the internal energy. Start by computing the specific volumes[12] and the Hugnoniot pressure and internal energy

$$V_0 \equiv 1/\rho_0 \ , \ V_Y \equiv 1/\rho_Y \ , \tag{7ab}$$

$$P_H = \frac{c_0^2 (V_0 - V_Y)}{\left[V_0 - s(V_0 - V_Y)\right]^2} \ , \text{ and} \tag{8}$$

$$E_H = \tfrac{1}{2} P_H (V_0 - V_Y) \, . \tag{9}$$

The thermodynamic state, at the yield point, is

$$P_Y = P_H + \frac{\Gamma}{V}(E_Y - E_H) \, , \tag{10}$$

and applying equation (6c) at the yield point gives the internal energy

$$E_Y = \tfrac{1}{2}(P_Y + \tfrac{2}{3} Y)(V_0 - V_Y) \, , \tag{11}$$

where the initial internal energy state is assumed to be zero.

---

[9] Li-Li Wang, **Foundations of Stress Waves**, Elsevier, Oxford, UK, First edition (2007). Equations (7.110a) and (7.110b), page 321.

[10] J. W. Forbes, **Shock Wave Compression of Condensed Matter: A Primer**, Springer-Verlag, Heidelberg, Germany (2012), pages 22-26, 153-157, and 183-184.

[11] **PAGOSA Physics Manual**, Section 6.6, pages 65-66.

[12] Density and specific volume are used interchangeably depending on the equation.

Substituting equations (9) and (10) into equation (11) and solving for the internal energy

$$E_Y = \tfrac{1}{2} P_H (V_0 - V_Y) + \left[\frac{Y}{3}\right] \frac{(V_0 - V_Y)}{1 - \frac{1}{2}\frac{\Gamma_0}{V_0}(V_0 - V_Y)}, \tag{12}$$

where $\Gamma / V = \Gamma_0 / V_0 = constant$ [13]. The resulting thermodynamic state for the elastic precursor

$$\begin{aligned} \rho_Y &\approx 8.9389344665 \text{ g/cm}^3 \\ E_Y &\approx 1.1138332696 \cdot 10^{-7} \text{ Mbar.cm}^3/\text{g} \\ P_Y &\approx 1.3903010384 \cdot 10^{-3} \text{ Mbar} . \end{aligned}$$

The solid total stress at the yield point is

$$\begin{aligned} \sigma_Y &= -P_Y + S_Y = -P_Y - \tfrac{2}{3} Y \\ &\approx -1.9903010384 \cdot 10^{-3} \text{ Mbar} . \end{aligned} \tag{13}$$

Note that PAGOSA computes the deviatoric stress (S_{ij}) and not the total stress[14] (σ_{ij}).

The elastic Rayleigh line connects the initial state to the yield point, Figure P2(a). The elastic precursor wave[15] velocity (U_{se}) can be computed from equations (6a) and (6b). It is

$$U_{se}^2 = V_0^2 \frac{[\![-\sigma_{xx}]\!]}{[\![V]\!]} , \tag{14}$$

The initial total stress is zero ($\sigma_{xx} = 0$). Then, the elastic precursor wave velocity is

$$U_{se} = V_0 \sqrt{\frac{-\sigma_Y}{V_0 - V_Y}} = V_0 \sqrt{\frac{P_Y + \frac{2}{3} Y}{V_0 - V_Y}} \approx 0.47221765470 \text{ cm}/\mu\text{s} . \tag{15}$$

The elastic precursor particle velocity, equation (6a), is

$$u_Y = \left(1 - \frac{V_Y}{V_0}\right) U_{se} \approx 4.7198162456 \cdot 10^{-4} \text{ cm}/\mu\text{s} . \tag{16}$$

This solution for the elastic precursor wave is compared to Udaykumar's solution in Table 2. The comparison is excellent.

[13] Using the Los Alamos historical standard practice of asserting that $\Gamma / V = constant$.
[14] **PAGOSA Physics Manual**, Section 14.1, page 131.
[15] The subscript *se* stands for shock and elastic.

Table 2. Elastic Precursor Wave Solution

name	*symbol*	*Udaykumar et.al.*	*Our Solution*	*units*[16]
Wave Velocity	U_{se}	0.4722	0.4722176547	cm/μs
Particle Velocity	u_Y	4.720	4.7198162456	m/s
Density	ρ_Y	8.9389	8.9389344665	g/cm^3
Internal Energy	E_Y	0.11138	0.1113833270	bar.cm^3/g
Pressure	P_Y	1.3903	1.3903010384	kbar
Deviatoric Stress	S_Y	-0.60	-0.6000000000	kbar
Total Stress	$\sigma_Y = -P_Y + S_Y$	-1.9903	-1.9903010384	kbar

The state of the material behind the plastic shock can be derived from the general Rankine-Hugoniot shock jump conditions. The state of the material after the elastic precursor has passed is denoted with subscript 2. The reference condition for this shock is the yield point, as shown in Figure P2(c). It is important to note that the reference point has a non-zero velocity, energy, and stress. The conservation of mass[17] is

$$\rho_2 = \rho_Y \frac{u_Y - U_s}{u_2 - U_s}. \tag{17}$$

The conservation of linear momentum[18] is

$$P_2 = P_Y + \rho_Y (U_s - u_Y)(u_2 - u_Y). \tag{18}$$

The conservation of energy, equation (6c), produces

$$E_2 = E_Y + \tfrac{1}{2}(P_Y + P_2 - 2S_Y)(V_Y - V_2). \tag{19}$$

The particle velocity in the plastic shock (u_2) is one-half [19] of the impact velocity since the impactor and the target are the same material. Therefore, the particle velocity is

$$u_2 \equiv \tfrac{1}{2}U_0 = 20 \text{ m/s} = 2.0 \cdot 10^{-3} \text{ cm/}\mu\text{s}. \tag{20}$$

The thermodynamic state of the plastic wave must also satisfy the Mie-Grüneisen equation of state written in terms of density instead of specific volume

$$P_{\text{EOS}}(\rho, E) = P_H + \Gamma\rho\,(E - E_H), \tag{21}$$

where

[16] Note that the table is not presented in a consistent set of units (e.g., internal energy and pressure).
[17] J.W. Forbes, **Shock Wave Compression of Condensed Matter: A Primer**, Springer-Verlag, Heidelberg, Germany (2012), page 20, equation (2.7).
[18] *Ibid.*, page 20, equation (2.8).
[19] *Ibid.*, page 41.

$$P_H = \frac{c_0^2 (V_0 - V)}{\left[V_0 - s(V_0 - V)\right]^2}, \text{ and} \tag{22a}$$

$$E_H = \tfrac{1}{2} P_H (V_0 - V). \tag{22b}$$

There are four equations and four unknowns. However, those equations are solely a function of the plastic shock velocity, U_s. The plastic shock velocity is the root of the equation

$$f(U_s) = P_2(U_s) - P_{\text{EOS}}[\rho_2(U_s), E_2(U_s)] = 0 \tag{23}$$

Solving[20] equation (23) results in the complete description of the plastic shock state. The root is

$$U_s \approx 0.39769567071 \text{ cm}/\mu\text{s}.$$

The resulting state for the plastic wave (ρ_2, E_2, P_2) is numerically

$$\rho_2 \approx 8.97345305522 \text{ g/cm}^3$$
$$E_2 \approx 2.13530160108 \cdot 10^{-6} \text{ Mbar.cm}^3/\text{g}$$
$$P_2 \approx 6.81592225573 \cdot 10^{-3} \text{ Mbar}.$$

This solution for the plastic shock wave is compared to Udaykumar's solution in Table 3. The comparison is excellent. Notice that the deviatoric stress S_{xx} is a single constant value for both waves. Why? The Hugoniot Elastic Limit (HEL) has been reached in all the space between the head of the elastic wave in the target and the tail of the elastic wave in the flyer. In contrast, the total stress is a different value in the two waves. The plastic stresses are

$$S_2 \equiv S_Y = -\tfrac{2}{3} Y = -0.6 \text{ kbar} \tag{24}$$
$$\sigma_2 = -P_2 + S_2 \approx -7.4159222557 \text{ kbar} \tag{25}$$

Table 3. Shock (Plastic) Wave Solution

name	*symbol*	*Udaykumar et.al.*	*Our Solution*	*units*[21]
Shock Velocity	U_s	0.3977	0.3976956707	cm/μs
Particle Velocity	u_2	0.0020	0.0020000000	cm/μs
Density	ρ_2	8.9735	8.9734530552	g/cm^3
Internal Energy	E_2	2.1353	2.1353016011	bar.cm^3/g
Pressure	P_2	6.8159	6.8159222557	kbar
Deviatoric Stress	S_2	-0.60	-0.6000000000	kbar
Total Stress	$\sigma_2 = -P_2 + S_2$	-7.4159	-7.4159222557	kbar

[20] One can solve the nonlinear equation by trial and error, graphical, bisection, secant method, Excel©, Mathematica©, or any other familiar technique.
[21] Note that the table is not presented in a consistent set of units (e.g., internal energy and velocity).

At $t = 170\ \mu\text{s}$ the leading edges of the two waves are located at:

$$x_{se} = U_{se}\, t \approx 80.2770013 \text{ cm} \qquad \textit{Elastic precursor wave}, \tag{26}$$

$$x_{s} = U_{s}\, t \approx 67.6082640 \text{ cm} \qquad \textit{Plastic shock wave}\ . \tag{27}$$

This completes the derivation of the analytic theory for the elastic precursor for the target. The shock wave structure in the flyer plate has not been solved. Be aware, the structure is not symmetric between the flyer and the target. For example, the elastic and plastic velocities are:

$$U_{se}\big|_{flyer} = U_0 - U_{se} \approx -0.4682176547 \text{ cm}/\mu\text{s}\,, \tag{28}$$

$$U_{s}\big|_{flyer} = U_0 - U_{s} \approx -0.3936947540 \text{ cm}/\mu\text{s}\,. \tag{29}$$

The corresponding shock locations, in the flyer, are:

$$x_{se}\big|_{flyer} \approx -79.5970013 \text{ cm}\,, \tag{30}$$

$$x_{s}\big|_{flyer} \approx -66.9281082 \text{ cm}\,. \tag{31}$$

In the next section the details of the PAGOSA implementation of the simulation are discussed.

PAGOSA Implementation

The copper body extends from $x = -100.0$ to $x = +100.0$ cm. The impact occurs at the $x = 0$ surface. A velocity of $U_0 = +0.004\,\text{cm}/\mu\text{s}$ is applied to the material for $x < 0$.

One material specification is used for the entire simulation. The simulation is constructed using two individual namelist bodies – one for the impactor and one for the target. The impactor body extends from half a cell in the negative *x* space (i.e., $x < 0$) and is assigned a positive velocity of 40 m/s = $4.0 \cdot 10^{-3}$ cm/μs. The target body extends over all the space that is not filled by the impactor (i.e., $x \geq 0$) and is assigned a zero velocity (the default). The consequence of this choice is that the simulation contains no interfaces. The PAGOSA interface reconstruction is not exercised in this simulation. Certainly the simulation could be performed with two materials, one for each of the bodies. That simulation would contain interfaces.

The **`exact_finish`** option is used so that the simulation stops at exactly 170 μs. In this way, the PAGOSA simulation results can be directly compared with the results of the analytic theory.

An extensive list of plot variables was chosen in this simulation. The density (**`dm`**), pressure (**`pm`**), internal energy (**`em`**), deviatoric stress component (**`Sxxm`**), and particle velocity (**`u`**) can be directly compared with the results from the analytic theory.

The material properties are taken from Table 1. The minimum pressure (**`pmin`**) is set to a large negative value so that no pressures are cutoff or limited. After the simulation, the absolute bounds of the material pressure can be checked. The pmin choice can then be confirmed as proper or not. Would it have mattered if we set **`pmin = 0.0`** in the simulation? The initial internal energy is set to zero (**`e0 = 0.0`**) so that the changes in internal energy can be easily determined.

Notice that not all the graphics dump variables (**`gd_var`**) are plotted by Ensight (**`es_var`**). Another **GD_ES** run will be necessary to post-process the previously omitted graphics variables. **PAGOSA** produced all the requested data in the graphics dump file. Any **GD_ES** run can select among the graphics dump variables for visualization.

Version 17.2 of PAGOSA was used in all the simulations. The associated PAGOSA Input Reference Manual is LA-CP-14-20250 (November 2014).

```
Elastic Precursor
5.0mm mesh, 40 m/s impact

&mesh
    ncellx = 200, 200, coordx = -100.0, 0.0, 100.0, npes_x = 2,
    ncelly =  19,  19, coordy =   -9.5, 0.0,   9.5, npes_y = 8 /

&options
    dt0          = 0.1,
    idgeom       = 2,
    symm         = 'Cartesian',
    ibc          = 1,1, 0,0, 0,0,
    exact_finish = true /

&outputs
    t           = 0.0, 170.0,
    dt          =        5.0,
    dump_freq   = 10,
    short_freq  =  1,
    gd_freq     =  1,
    gd_var      = 'vofm',   'dm',     'pm',     'em',     'q',
                  'sxxm',   'plstm',  'plwkm',  'strnm',  'eldem',
                  'yieldm', 'shearm', 'u',      'v',      'w',
    gd_mat      = 15*0,
    es_var      = 'slice',  'dm',     'pm',     'em',     'q',
                  'sxxm',   'plstm',  'plwkm',  'strnm',  'eldem', 'uvw',
    es_mat      = 11*0,
    es_last     = 35 /

Copper material
&mats
    material = 1,
    matbak   = 1,
    matname  = 'Cu',
    priority = 1,
    d0       = 8.93,
    e0       = 0.0,
    pmin     = -1.0,
    eosform  = 'usup',
    eoscon   = 0.394, 1.49, 0.0, 2.0, 0.0, 26.00,
    strform  = 'epp',
    y0       = 0.0009,
    g0       = 0.4500 /

&gen
    start_mode   = 1,
    restart_dump = true /
```

```
Copper impactor
&body
    material_number    = 1,
    surface_name       = 'plane',
    axis               = 'x',
    fill               = '-',
    xyz_translation_pt = 0.25, 0.0, 0.0,
    u0                 = 4.0e-03 /

Copper target
&body
    material_number    = 1,
    surface_name       = 'plane',
    axis               = 'x',
    fill               = '+',
    xyz_translation_pt = 0.25, 0.0, 0.0,
    u0                 = 0.0 /
```

Discussion

The first check should always be on the geometry and initial conditions. The **GEN** run output Short Edit gives:

	Ideal	**PAGOSA**	
Mass (kg)	33.93400	33.93398	~20 mg error
KE ($g.cm^2/\mu s^2$)	0.135736	0.135948	< 0.16% error
IE ($Mbar.cm^3$)	0.0	0.0	
Total Energy	0.135736	0.135948	< 0.16% error

The initial masses and energies are correct. The discrepancies can be easily explained by the choice of particle throw[22] in the **GEN** portion of the simulation. A default particle throw was used in this simulation (i.e., 5 coarse particles and 10 fine particles per direction per cell).

At the end of the simulation, $t = 170\ \mu s$, we have:

	Ideal	**PAGOSA**	
Mass (kg)	33.9340	34.04945	~115 mg error
Total Energy	0.135736	0.136042	< 0.23% error

The conservation of mass and energy is quite good for this simulation. The energy is partitioned between kinetic energy, internal energy, plastic work, and elastic distortional energy. PAGOSA has the capability of adding the elastic distortional energy to the internal energy (i.e., the `addelde` parameter in the `&options` namelist). We will return to this point in a few pages.

The plot variables, rendered in Ensight®, are shown in Figure P3. At the end of the simulation the waves moving to the left and right, away from the impact plane ($x = 0$), can be seen. The plot labelled 'Particle Velocity' is the PAGOSA x-component of velocity (`u`).

Figure P4 shows comparisons of the analytic theory and PAGOSA results for five variables. The plastic shock wave and elastic precursor can readily be perceived. The two shock fronts are smeared out over several cells due to the effects of artificial viscosity. Reducing the cell size will cause the two wavefronts to steepen and approach the analytic result. Would plotting the artificial viscosity (`q`) help in understanding the details of the wavefronts?

Figure P5 shows a detailed view of the elastic and plastic wavefronts. The comparison between theory and simulation is quite good. The internal energy is a little low in the elastic region in Figure P5(c). What if the elastic distortional energy was added to the internal energy? In Figure P5(d) the deviatoric stress S_{xx} is different in character in the elastic and plastic regimes. The elastic portion seems to be much smoother. What role does cell size play in this behavior?

[22] W. Weseloh, S. Clancy, and J. Painter, **PAGOSA Physics Manual**, Los Alamos National Laboratory, LA-14425-M (August 2010), Appendix B, Initial Volume Fraction Calculation.

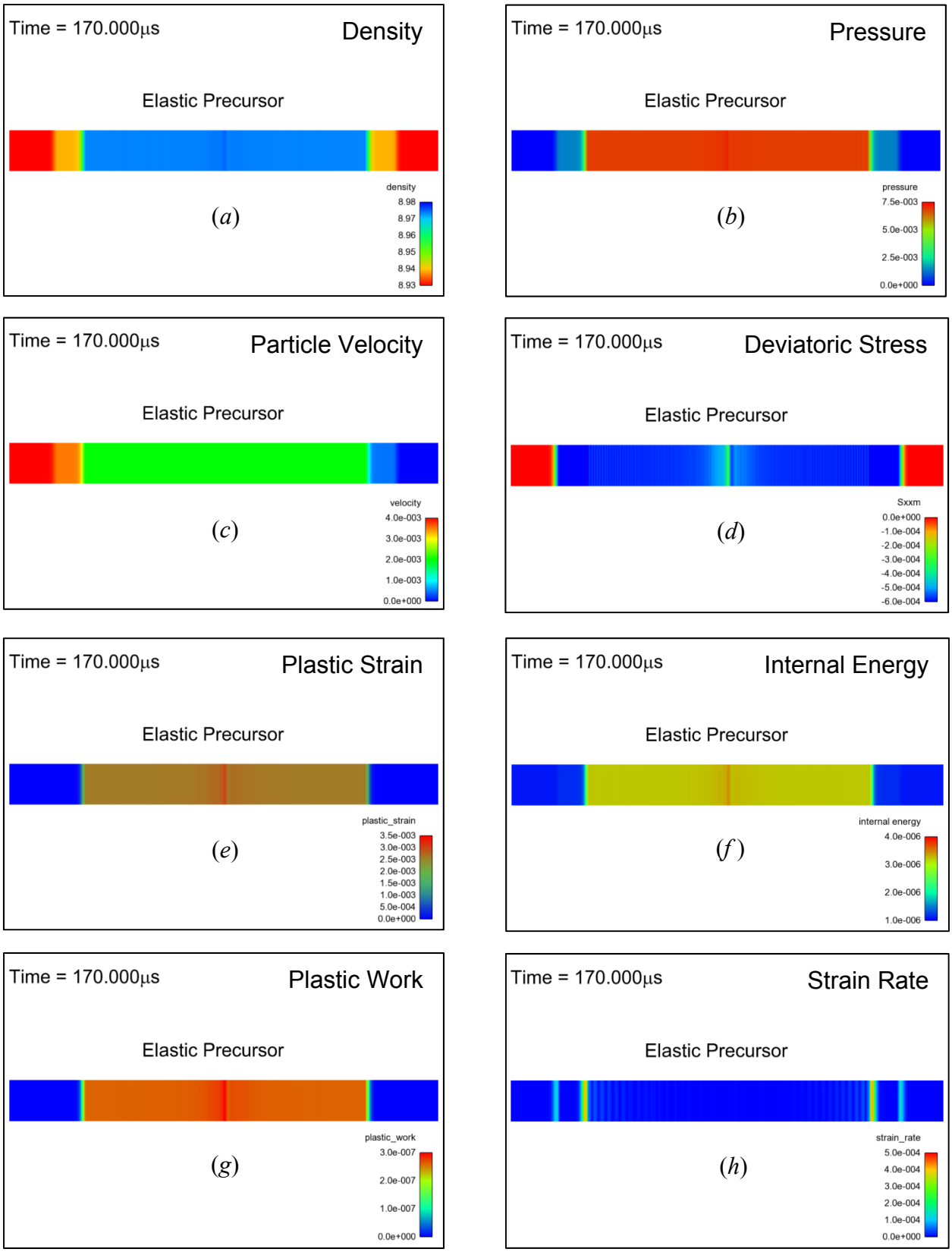

Figure P3. The PAGOSA simulation at 170μs. The plot variables: (a) density, (b) pressure, (c) velocity, (d) deviatoric stress component *x*-*x*, (e) plastic strain, (f) internal energy, (g) plastic work, and (h) strain rate.

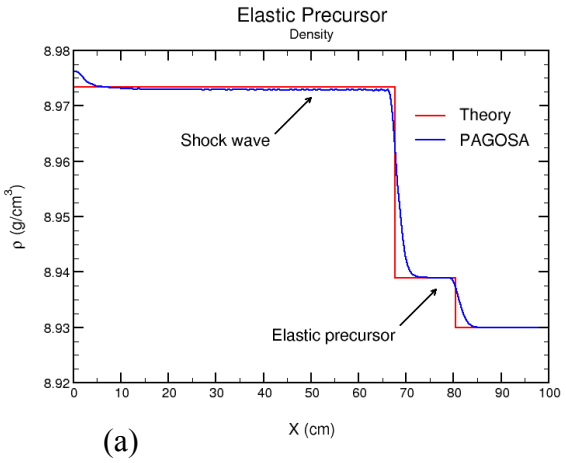

(a)

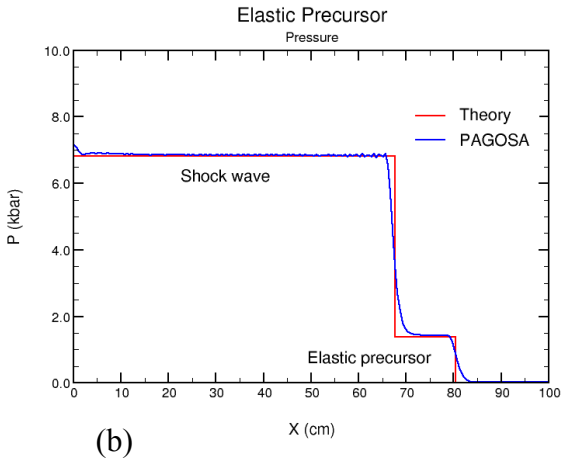

(b)

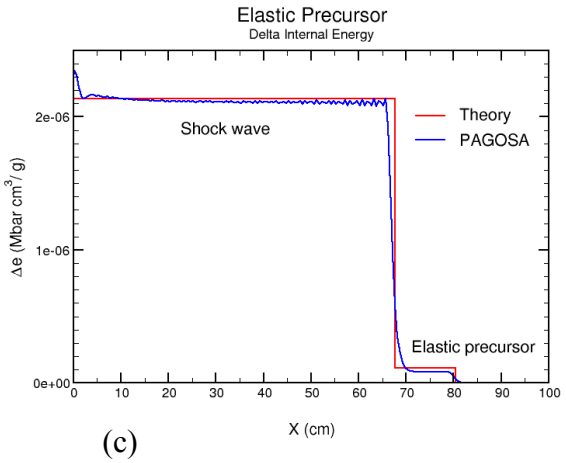

(c)

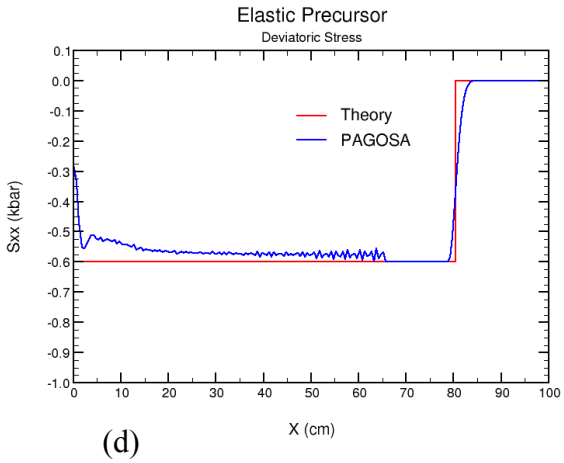

(d)

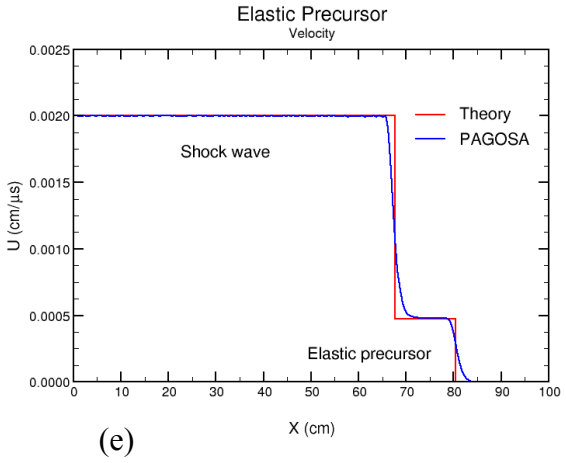

(e)

Figure P4. Comparison of the analytic theory and PAGOSA in the target material. The theory is shown by the red lines and the PAGOSA results are shown in blue for (a) density, (b) pressure, (c) internal energy, (d) deviatoric stress component *x*-*x*, and (e) the particle velocity.

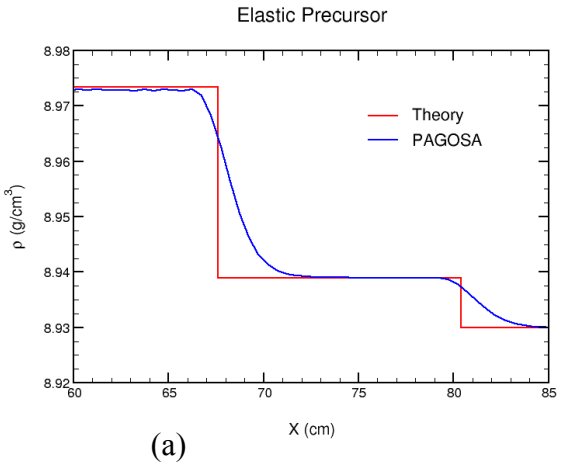

(a)

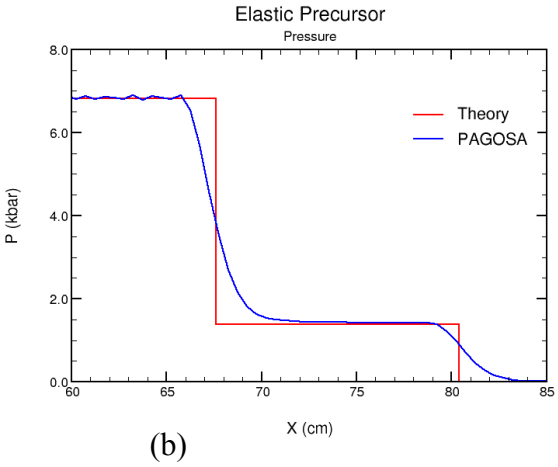

(b)

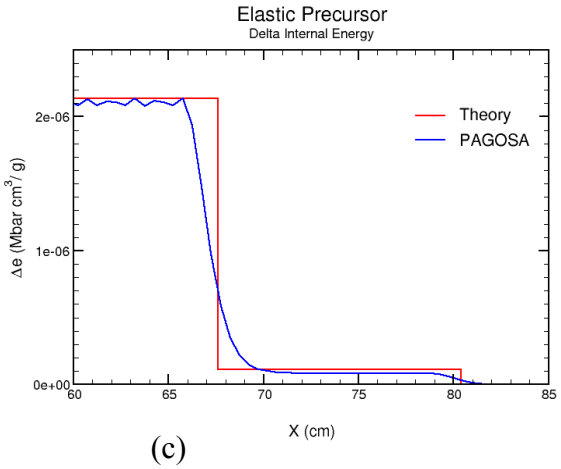

(c)

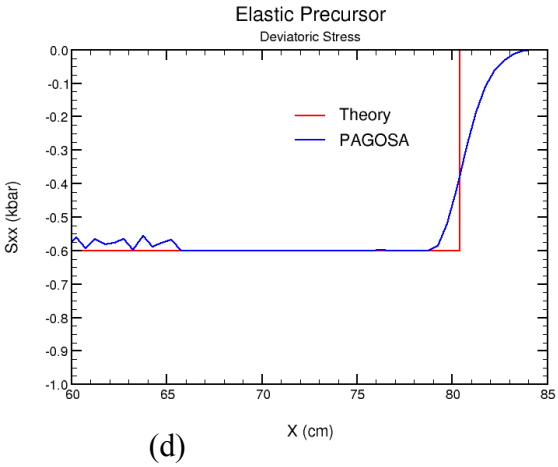

(d)

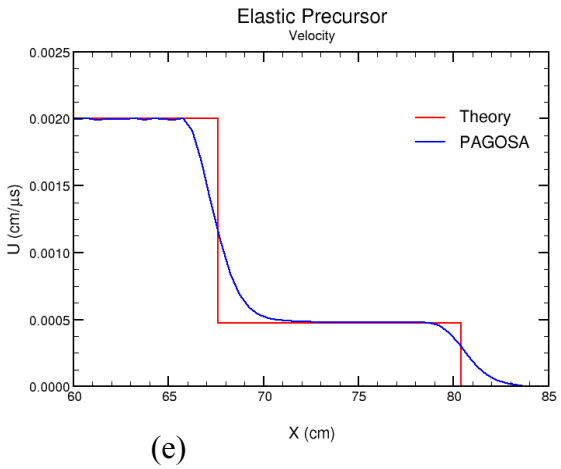

(e)

Figure P5. Comparison of the analytic theory and PAGOSA. An expanded view in the region of the two wavefronts is shown. The theory is shown by the red lines and the PAGOSA results are shown in blue for (a) density, (b) pressure, (c) internal energy, (d) deviatoric stress component *x*-*x*, and (e) the particle velocity.

Notice in Figure P5(c) that the internal energy in the elastic precursor is a little bit low. The difference is approximately $3 \cdot 10^{-8}$ Mbar.cm^3/g. To put that number in more familiar terms, the difference is less than 9 millikelvin. PAGOSA by default, and for historical reasons, does not include the elastic distortional energy[23,24] in the internal energy. It is computed and displayed in the Short Edits as a standalone quantity. However, an option in PAGOSA allows the user to add the elastic distortional energy to the internal energy for every cell and every timestep. Figure P6 shows the effect of adding the elastic distortional energy to the internal energy. The scale has been expanded to show the details of the internal energy distribution in the elastic precursor wave.

In many shock dynamic problems of interest the time spent in the elastic regime is quite short and neglecting the small amount of elastic energy is acceptable. However, in this simulation, that assumption is not true. For this simulation the elastic distortional energy matters.

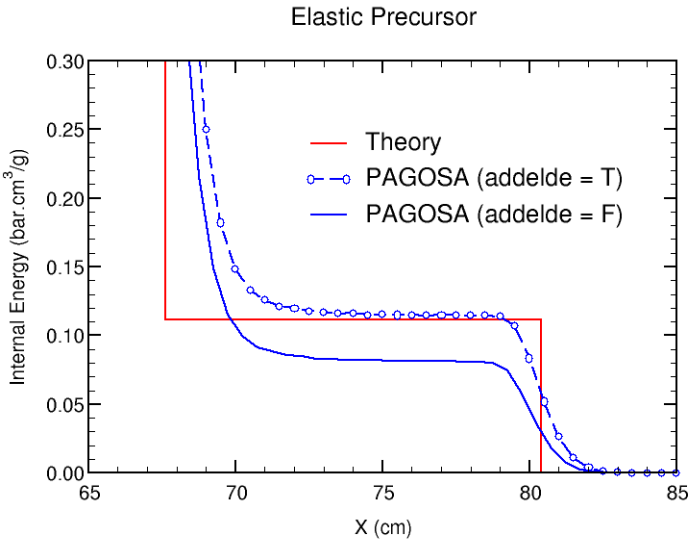

Figure P6. Comparison of the analytic theory and PAGOSA. An expanded view of the internal energy centered on the elastic precursor. The theory is shown in the red line. The solid blue line shows the original simulation. The dashed blue line shows the effect of adding the elastic distortional energy. The input parameter **addelde** is true (T) or false (F) depending on whether or not the elastic distortional energy is added to the internal energy. The circles on the dashed blue line are the raw PAGOSA data.

The PAGOSA simulation captures the leading edge of the elastic precursor in about 6 cells, the dashed blue line and blue points in Figure P6. The plastic wave, on the other hand, requires about 10 to 12 cells to resolve the sharp discontinuity.

A few exercises are suggested in the next section.

[23] **PAGOSA Physics Manual**, LA-14425-M. Appendix J.5 *Elastic Distortional Energy*, page 212.
[24] **PAGOSA Input Reference Manual**, Code Version 17.2, LA-CP-14-20250, Los Alamos National Laboratory (November 2014), pages 27-28 and 270-271.

Exercises

- Run a simulation with a new impact velocity, $U_0 = 2000$ m/s $= 0.2$ cm/μs. This is a case where the plastic shock has overtaken the elastic precursor. Udaykumar *et. al.* give a solution to this case. Check that solution.

- Continue the derivation presented in the theory section for the following variables

Deviatoric Stress: S_{yy}, S_{zz}, and S_{xy}.	(PAGOSA Physics Manual, equations 1.3)
Equivalent Plastic Strain: e^P	(PAGOSA Physics Manual, equation 14.30)
Plastic Work: W^P	(PAGOSA Physics Manual, equation J.6)

  Compare the newly derived analytic variable results with the PAGOSA simulation. Create plots in the form and style of Figure P5(a)-(e).

- Rerun the PAGOSA simulation with different cell size. As an example, a comparison of particle velocity profile for two different cell sizes is shown below.

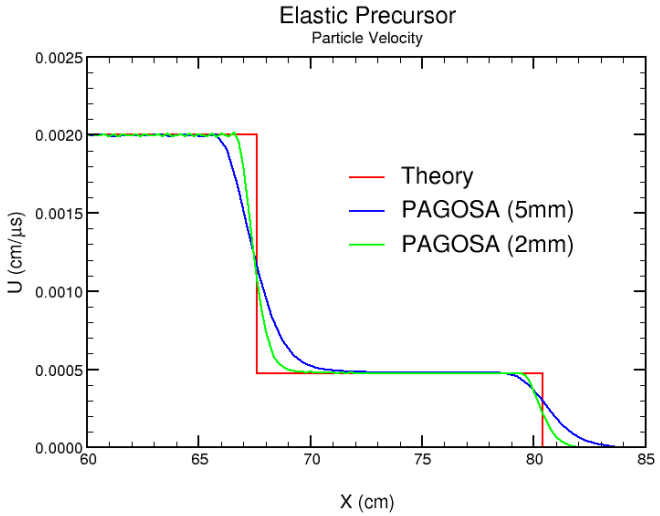

- Udaykumar *et. al.* explored the convergence of the solution with cell size [Figure 12 and equation (72) on page 163]. What is PAGOSA's L1 convergence rate?

- Try a two material simulation. Construct a PAGOSA simulation with two identical copper materials and two bodies, one per material. How is this simulation (*now exploiting material interface reconstruction*) different from the original simulation? Are the results significantly different?

- What is the critical velocity corresponding to transition shown in Figure P2(d)? Hint: $U_0 \approx 0.104176$ cm/μs and $x_{se} = x_s \approx 80.277$ cm.

Appendix: Wave Velocities and Elastic Moduli

The wave velocities are deeply related to the material elastic constants. For example, the elastic longitudinal velocity (c_L) is

$$c_L = \sqrt{\frac{\kappa + \frac{4}{3}G}{\rho_0}} \ ,$$

where κ is the bulk modulus. If the elastic precursor wave velocity is identified as the elastic longitudinal velocity[25], then the bulk modulus can be derived

$$\kappa = \rho_0 U_{se}^2 - \tfrac{4}{3}G \approx 1.3913 \text{ Mbar} .$$

A National Bureau of Standards (NIST) reference report[26] gives the bulk modulus of copper as 1.376 ± 0.002 Mbar, an error of about +1.11%. The shear modulus of copper used in this sample problem (G = 0.450 Mbar) is slightly different than the value reported in the 1974 NIST report (G = 0.454 ± 0.012 Mbar).

The shear wave velocity is defined as

$$c_S = \sqrt{\frac{G}{\rho_0}} \ ,$$

and the Poisson ratio of copper can be computed[27]

$$\nu = \frac{\frac{1}{2} - (c_S / c_L)^2}{1 - (c_S / c_L)^2} \approx 0.35402 .$$

The NIST report[28] gives the Poisson ratio as 0.350 ± 0.009, an error of about +1.14%.

Remember that neither the bulk modulus nor Poisson's ratio appear in the PAGOSA input.

Other elastic constants can be derived from the other various wave velocities.

[25] Forbes, page 152, equation (6.17).
[26] H.M. Ledbetter and E.R. Naimon, *Elastic Properties of Metals and Alloys II Copper*, **Journal of Physical and Chemical Reference Data**, Volume 3, Issue 4 (October 1974), 897-935. See Table 2, page 908.
[27] D.R. Christman, W. M. Isbell, S. G. Babcock, *Dynamic Properties of Materials, Volume V, OFHC Copper*, Materials and Structures Laboratory, General Motors Corporation, General Motors Technical Center, Warren, Michigan, Report MSL-70-23, Volume V (July 1971). See Appendix A and page 80.
[28] Ledbetter and Naimon. See Tables 9 and 10, page 923.

References

The elastic precursor sample is taken from the journal article:

H.S. Udaykumar, L.Tran, D.M. Belk, and K.J. Vanden, *An Eulerian Method for Computation of Multimaterial Impact with ENO Shock-Capturing and Sharp Interfaces*, **Journal of Computational Physics**, Volume 186 (2003), pages 136-177. See section 7.2: *Impact on elasto-plastic material*, pages 155-163.

Four excellent references for wave propagation are:

D.S. Drumheller, **Introduction to Wave Propagation in Nonlinear Fluids and Solids**, Cambridge University Press, Cambridge UK (2008), pages 170-189, 192-199, 230, 359-377, and 411-419.

J. W. Forbes, **Shock Wave Compression of Condensed Matter: A Primer**, Springer-Verlag, Heidelberg, Germany (2012), pages 22-26, 153-157, and 183-184.

Li-Li Wang, **Foundations of Stress Waves**, Elsevier, Oxford, UK, First edition (2007), pages 31, 267-279, and 290-324.

Ya. B. Zeldovich and Yu. P. Raizer, **Physics of Shock Waves and High Temperature Hydrodynamic Phenomena**, Dover Publications, New York (2002), pages 705-710, and 732-746.

Copper's dynamic properties are detailed in:

D.R. Christman, W. M. Isbell, S. G. Babcock, *Dynamic Properties of Materials, Volume V, OFHC Copper*, Materials and Structures Laboratory, General Motors Corporation, General Motors Technical Center, Warren, Michigan, Report MSL-70-23, Volume V (July 1971).

W.M. Isbell, F.H. Shipman, and A.H. Jones, *Hugoniot Equation of State Measurements for Eleven Materials to Five Megabars*, MSL-68-13, Materials & Structures Laboratory, General Motors Corporation (December 1968).

D.J. Steinberg, *Equation of State and Strength Properties of Selected Materials*, UCRL-MA-106439 Change 1, Lawrence Livermore National Laboratory (February 13, 1996).